The Journal of Experimental Biology 209, 4339-4354
Published by The Company of Biologists 2006
doi:10.1242/jeb.02517

A 'bright zone' in male hoverfly (*Eristalis tenax*) eyes and associated faster motion detection and increased contrast sensitivity

Andrew D. Straw[1,*], Eric J. Warrant[2] and David C. O'Carroll[1]

[1]*Discipline of Physiology, School of Molecular and Biomedical Science, The University of Adelaide, SA 5005, Australia and* [2]*Vision Group, Department of Cell and Organism Biology, Lund University, Lund, Sweden*

*Author for correspondence at present address: California Institute of Technology, Bioengineering, Pasadena, CA 91125, USA (e-mail: astraw@caltech.edu)

Accepted 29 August 2006

Summary

Eyes of the hoverfly *Eristalis tenax* are sexually dimorphic such that males have a fronto-dorsal region of large facets. In contrast to other large flies in which large facets are associated with a decreased interommatidial angle to form a dorsal 'acute zone' of increased spatial resolution, we show that a dorsal region of large facets in males appears to form a 'bright zone' of increased light capture without substantially increased spatial resolution. Theoretically, more light allows for increased performance in tasks such as motion detection. To determine the effect of the bright zone on motion detection, local properties of wide field motion detecting neurons were investigated using localized sinusoidal gratings. The pattern of local preferred directions of one class of these cells, the HS cells, in *Eristalis* is similar to that reported for the blowfly *Calliphora*. The bright zone seems to contribute to local contrast sensitivity; high contrast sensitivity exists in portions of the receptive field served by large diameter facet lenses of males and is not observed in females. Finally, temporal frequency tuning is also significantly faster in this frontal portion of the world, particularly in males, where it overcompensates for the higher spatial-frequency tuning and shifts the predicted local velocity optimum to higher speeds. These results indicate that increased retinal illuminance due to the bright zone of males is used to enhance contrast sensitivity and speed motion detector responses. Additionally, local neural properties vary across the visual world in a way not expected if HS cells serve purely as matched filters to measure yaw-induced visual motion.

Key words: insect vision, motion detection, sexual dimorphism.

Introduction

Local properties of fly eyes

From the first published drawing of a magnified fly's head (Hooke, 1665), it has been clear that facet lenses are often not uniform in size across the compound eye. Insects, like other animals including humans, sample the visual world with sensitivity and resolution that vary across space. In general, it may be difficult to ascribe specific functionality to these regionalized properties because the same compound eyes and ocelli must serve a variety of visual behaviors. One success at ascribing specific functionality arose from the discovery of sexual dimorphism in the retina of muscoid flies *Calliphora vicina* and *Musca domestica*. Males have an 'acute zone' in the fronto-dorsal portion of the visual world where the angle between adjacent ommatidial axes ($\Delta\phi$) is nearly half that in the lateral eye (Land and Eckert, 1985). Males keep the image of females they are pursuing in this region (Boeddeker et al., 2003; Wagner, 1986; Wehrhahn, 1979), and the male acute zone is thought to be an optical specialization for detection and tracking of females. This region of increased angular resolution comes at a significant cost. To overcome limits on spatial resolution due to optical diffraction, increased angular resolution demands not only more facets with smaller interommatidial angles but also larger facet diameter, leading to a significant increase in eye size (Kirschfeld, 1976; Land, 1997; van Hateren, 1989).

Large lenses are not the only investment made by male muscoid flies in the region of the acute zone. Additional, sex-specific '7r' photoreceptors appear to have been modified from the typical R7 receptors to have properties similar to those of R1–6, creating a 7% increase in signal-to-noise by contributing to the same postsynaptic cells (Franceschini et al., 1981; Hardie, 1983; Hardie et al., 1981). The R1–6 photoreceptors in this region have finer angular sensitivity, are faster by ~20%, and have a higher metabolic cost than lateral photoreceptors (Burton et al., 2001; Hornstein et al., 2000). Furthermore, there are several male-specific interneurons with receptive fields in this region (Hausen and Strausfeld, 1980).

Functionally, these properties all appear to be adaptations for detecting and chasing small targets, namely conspecific females.

Historically, several design principles have been used to explain properties of eyes and neurons, including maximizing information transmission, minimizing redundancy, exploiting statistical correlation, and reducing unnecessary energy expenditure (Burton et al., 2001; de Ruyter van Steveninck and Laughlin, 1996; Laughlin, 1981; Laughlin et al., 1998; Srinivasan et al., 1982). Thus, acute zones indicate that demand for information is not uniform across visual space, and their presence suggests that some regions of the visual world are particularly important for specific behaviors. More generally, different behaviors may require different information from the visual system. While at the optical and photoreceptor level it seems that specializations such as increased contrast sensitivity and spatial resolution would be beneficial for any behavior, these specializations come with at least one additional cost – that of increased eye size and mass. Thus, a functional adaptation to serve one behavior may compromise performance of other tasks. For later stages of visual processing, such as motion detection, it is unclear whether a single set of elementary motion detectors (EMDs) might serve as the basis for both visual course correction and target chasing behaviors with potentially conflicting demands or whether estimates of visual motion may be computed independently.

Local properties of fly motion detection and the 'matched filter hypothesis'

How does non-uniform visual sampling affect the properties of visual interneurons and behavior? Fly lobula plate tangential cells (LPTCs) are neurons sensitive to visual motion over a large portion of the visual world. In the muscoid flies *Calliphora*, *Musca* and *Phaenecia*, the large receptive fields of LPTCs have non-uniform directional selectivity (Hausen, 1982; McCann, 1974), and the local preferred directions (LPDs) of these neurons appear matched to particular components of optic flow induced by particular types of self-motion such as rotation about particular axes (Krapp et al., 1998; Krapp and Hengstenberg, 1996; Krapp et al., 2001). This has increased interest in the concept of motion-matching, whereby optic flow may be estimated by the correlation of local motion direction and velocity with the local response properties within large receptive fields (Bülthoff et al., 1989). As shown by Krapp and colleagues, the distribution of directions of local motion experienced across the visual world during, for example, roll rotation, are similar to the LPDs of fly VS (vertical system) cells. Combined with extensive work on other cell classes, this work provides a compelling explanation for the receptive field structure of fly LPTCs. These cells may be 'matched filters' for specific components of self-motion induced optic flow, such as yaw rotation, roll rotation and forward translation. Furthermore, modeling efforts have shown that biologically inspired models based on such matched filters can accurately estimate the components of optical flow due to self translation and rotation in a rapid, feed-forward manner (Dahmen et al., 2001; Franz et al., 2004; Franz and Krapp, 2000). In other flies, the LPD organization is largely unknown, although the subject is of inherent interest because anatomical (Buschbeck and Strausfeld, 1997) and physiological (O'Carroll et al., 1996; O'Carroll et al., 1997) characteristics of LPTCs vary in a correlated manner with visual behavior. Yet small-field motion-sensitive neurons of the medulla and pre-synaptic to LPTCs are highly conserved at the anatomical level (Buschbeck and Strausfeld, 1996), suggesting that the anatomy and physiology of LPTCs may have high 'evolutionary plasticity' that underlies behavioral differences between groups within the flies.

The remarkable similarity in the local preferred directions of LPTCs with the predicted patterns of local velocities during different types of self-motion raises the question of how other local properties of LPTCs might be correlated with visual input. In particular, local velocity tuning is a critical factor when assessing whether LPTCs may act as matched filters. Previous experiments used a spot moving in a small circular orbit at constant angular velocity repeated in each of many locations over the receptive field to measure both the local preferred direction and the 'local motion sensitivity', the magnitude of response modulation to this particular stimulus (Krapp and Hengstenberg, 1997). Yet the velocity tuning of these neurons remains unclear because these cells behave locally much like EMDs of the correlator type, in which output is not proportional to velocity *per se*, but instead to a combination of spatial and temporal frequencies and contrast (Egelhaaf and Borst, 1993; Egelhaaf et al., 1989). Furthermore, differences in local contrast sensitivity and local gain also affect the physiological properties of these cells. Without information on these properties and their variation across the receptive fields of these neurons, the local responses of fly LPTCs will be difficult to predict for arbitrary moving patterns. With such data, however, increasingly accurate predictions of the responses to velocity can be made (Boeddeker et al., 2005; Dror et al., 2001; Lindemann et al., 2005; Shoemaker et al., 2005).

In this study, we found that male *Eristalis tenax* hoverflies have a 'bright zone' similar to that of the blowfly *Chrysomia megacephala* (van Hateren et al., 1989), which results in increased light capture but is not accompanied by large changes in interommatidial angle. Additionally, we sought investigate *Eristalis* LPTCs in the context of the matched filter hypothesis and to explore the effect of the male-specific bright zone on the performance of these motion detecting neurons. To do so, we developed a stimulus that allows exploration of the local spatial-, temporal- and contrast-sensitivity of wide-field motion detecting neurons and used it to investigate *Eristalis* HS cells. Furthermore, as part of the characterization of the local properties of *Eristalis* LPTCs, we performed an analysis that allowed us to determine the relative contribution of Type 1 and Type 2 EMDs, those with inputs from neighboring ommatidia and next-but-one neighbors, respectively (Buchner, 1976; Buchner, 1984).

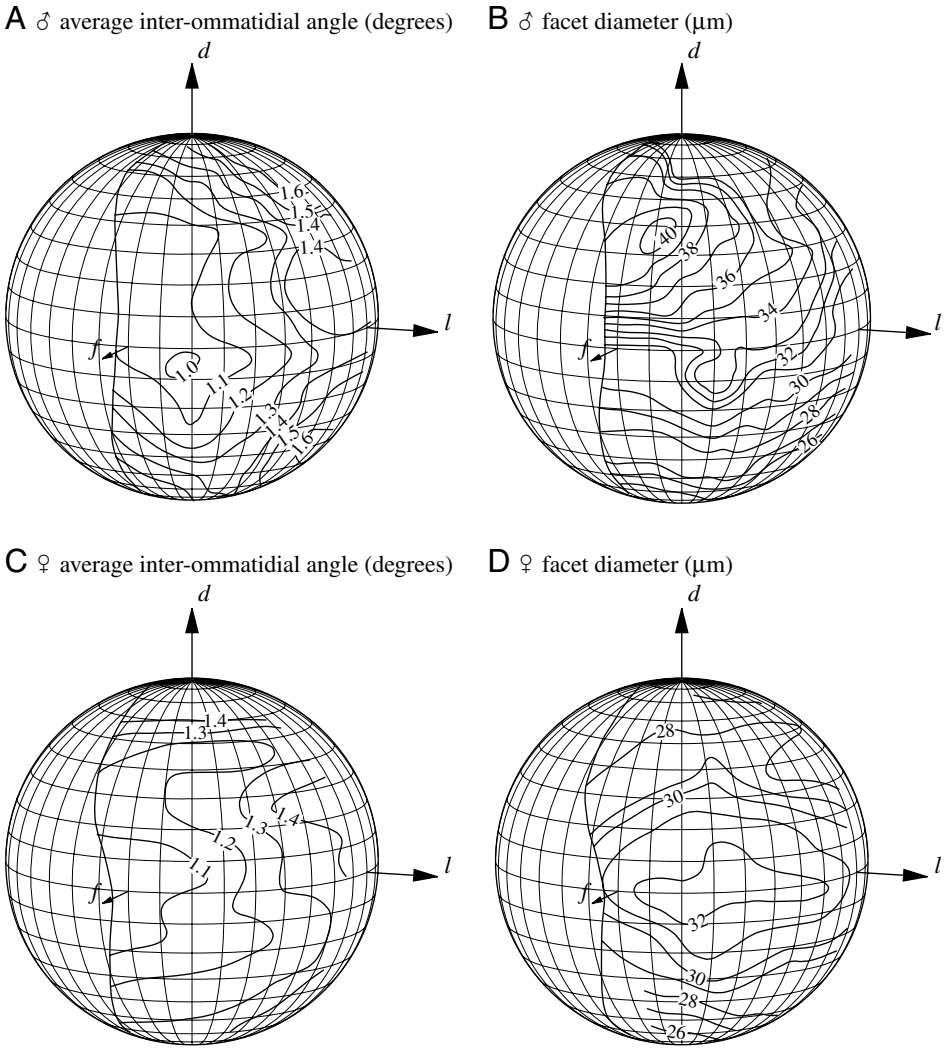

Fig. 1. Optical characteristics of *Eristalis tenax* eyes showing the 'bright zone' of males, in which facet diameter is maximal in the fronto-dorsal eye but is not associated with smallest interommatidial angle. Interommatidial angles are given as the average of the angles across horizontal and vertical sampling baselines. Data are from a single male and single female fly and in close agreement with data from the other fly tested of each sex. *f*=frontal, *d*=dorsal, *l*=lateral.

Materials and methods

Optics

The method used to map interommatidial angles in the visual field followed standard procedures (Land and Eckert, 1985; Rutowski and Warrant, 2002) and was performed on two male and two female flies. Briefly, the small end was cut from a plastic pipette tip leaving an opening large enough for a fly's head to protrude through. The fly was fixed in position by gluing the proboscis to the tube with dental wax, and this preparation was then mounted at the centre of curvature of a Leitz goniometer (Wetzlar, Germany). The goniometer was placed onto the foot-plate of an Askania macroscope (Rathenow, Germany). It was then manipulated so that the flat posterior eye edge was parallel to the plane of the stage. The head was further manipulated so that (1) the origin of the three goniometer axes was in the centre of the head, and (2) the three goniometer axes were lined up with the dorsal–ventral (yaw), anterior–posterior (roll) and left–right (pitch) axes, respectively, of the fly's head. With the stage horizontal, both eyes then looked vertically upwards into the objective of the macroscope, and when observed in this position, the eyes were oriented exactly anteriorly (from the animal's point of view). The goniometer allowed us to tilt the stage (and thus the head) in defined angular steps of elevation and azimuth, with elevation=0° and azimuth=0° defined as the anterior orientation described above (*f* in Fig. 1). Dorsal (*d*) corresponds to an elevation of +90° and lateral (*l*) to an elevation of 0° and azimuth of +90°. The exact anterior coordinates (azimuth=elevation=0°) were confirmed when observing the deep pseudopupil whose appearance in both eyes is mirror-symmetrical along the eye equator (Franceschini, 1975).

To illuminate the eyes we introduced a half-silvered mirror, angled at 45°, just beneath the objective of the macroscope. Collimated white light (from a halogen source) was directed laterally to the mirror so that the eyes were illuminated and viewed along the same axis ('orthodromic illumination'). This type of illumination reveals a luminous pseudopupil. Using chalk dust sprinkled lightly on the eye to provide landmarks, we took a series of photographs of the luminous pseudopupil in the left eye at 10° intervals of elevation and azimuth. Due to the structure of the apparatus we could not go beyond elevations of +70° or –70° or an azimuth of 80°.

Hence, our observations of the appearance and location of the pseudopupil were restricted to the frontal region of the eye, which is, in the context of our study, the region of greatest interest.

From each photograph we were able to determine the facet coordinates of the facet found at the centre of the pseudopupil, using the landmarks as a guide. Using established formulae that correct for elevation distortions in the projection (Land and Eckert, 1985), we calculated the average local interommatidial angle ($\Delta\phi$) and facet diameter (D) for each combination of elevation and azimuth. These data were plotted on a sphere representing 3D space around the animal, and contours were interpolated to connect regions of space viewed by parts of the eye with the same average local $\Delta\phi$.

Electrophysiology

Lobula plate tangential cells (LPTCs) of wild-caught hoverflies *Eristalis tenax* L. were recorded intracellularly. All recordings were done from the left lobula plate, and the responses described are from ipsilateral receptive fields. Electrodes were pulled on a Sutter P-97 puller (Novato, CA, USA) and filled with 2 mol l^{-1} KCl, and had tip resistances of 20–40 MΩ. The calibration of 3D position and orientation was done with reference to morphological features of the fly head, using the planar back surface of the head and the animal's midline to define the vertical and longitudinal axes of the animal's head, respectively.

Stimulus

Stimuli were displayed on a CRT (LG Flatron 915 FT+; Seoul, S. Korea) updated at 200 Hz with a mean luminance of 41 cd m^{-2} under the control of a ×86 PC running Windows 2000 with an nVidia graphics card and drivers. The flat screen of our CRT was placed close enough to the fly to subtend an approximately 100° horizontal field of view. The Vision Egg stimulus generation software library (made freely available by A.D.S. at www.visionegg.org), was used to generate and display Gaussian windowed (s.d.=7.1°) sinusoidal gratings (Gabor wavelets) corrected with perspective distortion calibrated according to each fly's position. Thus, from the fly's location, a specified spatial wavelength subtended exactly the same angle regardless of screen position. Similar stimuli can be produced by the 'mouse_gabor_perspective' demonstration program distributed with the Vision Egg.

Calculating local preferred directions and local motion sensitivity

To characterize neurons encountered in the present study, we measured local preferred direction using a sinusoidal grating method adapted from O'Carroll et al. (O'Carroll et al., 1997) (Fig. 2C)]. A localized grating near the spatial and temporal frequency optimum of the cells under study (0.1 cycles $deg.^{-1}$, 5 Hz) was used (other grating parameters as described above). Following presentation of a mid-luminance gray screen, an initial 3 s period of motion at 180° (leftward) was shown in an attempt to ensure that any effects due to motion adaptation would be similar in different trials and that the cell was in a consistent state prior to further stimulation. The stimulus consisted of a series of 16 motion directions presented in sequence, each for 200 ms and at a 22.5° increment from the previous direction. In this way, 16 sequentially tested directions mapped out local directional tuning. To further minimize the possibility that motion adaptation corrupted the local preferred direction (LPD) estimate, the direction of motion was changed in a clockwise manner initially and then in the counter-clockwise direction in a second, otherwise equivalent trial. The LPD was calculated separately for the clockwise and counter-clockwise trials by fitting with a cosine function (using a simplex error minimization routine), which accurately describes the direction tuning of LPTCs (Hausen, 1982; van Hateren, 1990) as described by the function:

$$R(\theta) = A_{LMS}\cos(\theta-\theta_{LPD}) . \quad (1)$$

A_{LMS} is the amplitude of modulation, or local motion sensitivity (LMS), and θ_{LPD} is the phase offset, or local preferred direction (LPD).

Estimating contrast–response and contrast sensitivity

The primary means of determining the contrast–response relationship in this study was with a 'contrast ramp' (O'Carroll, 2001; O'Carroll et al., 1997). In control experiments (e.g. Figs 3, 4), the validity of this approach was confirmed by a contrast step technique, which has been used in earlier studies of contrast sensitivity in the fly (Dvorak et al., 1980; Srinivasan and Dvorak, 1980).

Contrast steps were performed for moving, Gaussian-windowed sinusoidal gratings at a given spatial and temporal frequency after exposure to a mean gray screen for at least 3 s. The response to 2 s of motion of a contrast specified at the center of the stimulus patch was recorded. The primary difficulty of this method is selecting an appropriate time window for analysis. The onset time-course of LPTC responses depends on the temporal frequency of the input but approaches steady-state with a time constant equal to that of the delay filter in a correlator model (Egelhaaf and Borst, 1989); however, later portions of the response are reduced by motion adaptation (Maddess and Laughlin, 1985). By taking the mean membrane potential from 50 to 150 ms after the onset of stimulation, we attempted to minimize effects of motion adaptation while measuring steady-state responses. Because the response of *Eristalis* HS cells are well fit by a correlator model with a time constant of approximately 35 ms (Harris et al., 1999), onset transients should be minimal during this period. Despite the attempt to overcome these issues when dealing with the contrast step method, it seems that adaptation will always make analysis of step responses problematic (O'Carroll, 2001), at least when attempting to characterize the response of unadapted motion detectors, as in this study.

A contrast ramp stimulus is faster than the step technique in determining the contrast–response relationship because it sweeps through a range of monotonically increasing contrasts

in a short period of time. In this study, we used 1 s ramps given by the equation:

$$C(t) = At + Bt^{n} \ , \quad (2)$$

where t is time (s), A=0.3, B=0.7, n=10. With these values, contrast rises approximately linearly for about 0.6 s to a value of near 0.2 and then rapidly increases to a final value of 1.0. We argue that this method reduces errors in the contrast–response measurement because contrast is always increasing and motion adaptation is thought to be contrast sensitive (Harris et al., 2000). Thus, response at any moment will only be affected by any potential motion adaptation resulting from stimulation at prior lower contrasts. Furthermore, the total stimulus duration is relatively brief, further limiting the effect of adaptation. The effect of onset transients should also be minimized because there is no sudden onset luminance step.

In an effort to overcome the effects of 'noise' (response variability due to pattern sensitivity, neural response variability, and measurement errors), each ramp was presented at least three times at a randomized starting phase. The average of these responses was computed, transformed from the time domain to a logarithmic contrast domain, and fit with a Weibull cumulative distribution function. The transformation to the logarithmic contrast domain subtracted an estimated neural latency. For the results presented here, a value of 15 ms was found to provide the best fit between contrast ramp data and contrast step data. Before fitting the data, it was 'padded' with zero response values in the very low contrast range (<0.01) to force the fit to have a near zero value at low contrast. The Weibull function was chosen for its ability to fit a wide range of monotonically increasing functions with only a gain term and two other parameters, which were computed with a simplex error minimization routine.

The resulting fits were used to compute contrast sensitivity, a unitless value equal to the reciprocal of the threshold contrast required to evoke a criterion response. For this study, a fixed criterion response value of 2 mV above the resting potential was used as a threshold, analogous to the fixed criterion used by Srinivasan and Dvorak (Srinivasan and Dvorak, 1980). Other authors have used a 'detectability criterion', e.g. a response criterion of a just noticeable (to the experimenter) difference (Dvorak et al., 1980) or the standard deviation of the resting membrane potential of the cell (O'Carroll et al., 1997). In preliminary experiments, we verified that no qualitative shifts were observed when the criterion was half of the usual value (although lower criteria yield higher sensitivity values). Changing the criterion within a low-response range seemed primarily to be a trade-off between noise and high sensitivity, and thus the present approach seems equally valid to detectability-based analyses.

Estimating contributions from Type 1 and Type 2 EMDs

In the spatial domain, correlator models are highly constrained by the hexagonal spacing of the input. This property has been previously exploited to provide confirmation of the validity of the correlator model in application to fly optomotor responses (Buchner, 1976; Buchner, 1984; van Hateren, 1990) and to directly compare the sampling distance of fly LPTCs with the spacing of ommatidia (Schuling et al., 1989; Srinivasan and Dvorak, 1980). We used this property combined with the known angular spacing of *Eristalis* ommatidia (Fig. 1A,C) to estimate the relative contributions of the EMD types 1 and 2 (with inputs from neighboring ommatidia and next-but-one neighboring ommatidia, respectively). Responses in the spatial-frequency domain were fit with a two-EMD correlator model with three free parameters using a simplex error minimization routine. Only a single free parameter, the relative contribution from the EMD types, controls the most critical feature of the model, the location of the zero crossing and the nearby sharp rolloff.

The response of the model is given by:

$$R(F_s) = k\tanh\{s[g_1E_1(F_s) + g_2E_2(F_s)]\} \ , \quad (3)$$

where the response R is given as a function of spatial frequency F_s. The overall gain is set by the parameter k, while the tanh function and the parameters s were necessary to model saturation at high contrasts. The relative contributions of Type 1 and Type 2 correlators are given by g_1 and g_2, which were under the control of a single free parameter. The response of each EMD is found with a simplified analytic correlator model in the spatial domain using the formulation given elsewhere (Dror et al., 2001). In this context, because contrast and temporal frequency are constant for any fit, these factors are implicitly included in the parameters fit above and are removed from the model used:

$$E_n(F_s) = \sin(2\pi F_s n\Delta\phi_h)\mathrm{MTF}(F_s) \ , \quad (4)$$

where n is 1 or 2, corresponding to the EMD type. $\Delta\phi_h$ is the angular separation in the direction of correlation calculated from $\Delta\phi$, the interommatidial angle shown in Fig. 1, by the relation $\Delta\phi_h=\cos(30°)\Delta\phi$. The modulation transfer function $\mathrm{MTF}(F_s)$ approximates the low-pass filtering properties of the optics, and we used a Gaussian angular sensitivity function of the form given by (Götz, 1964):

$$\mathrm{MTF}(F_s) = \exp[-3.56(\Delta\rho F_s)^2] \ , \quad (5)$$

where $\Delta\rho$ is the acceptance angle. This was calculated using the approximation $\Delta\rho\approx\Delta\phi$, which is the relation determined from electrophysiological measurements of $\Delta\rho$ in *Chrysomyia* (van Hateren et al., 1989) and is similar to the relationship between electrophysiologically measured *Eristalis* angular sensitivity functions (James, 1990) and the data of Fig. 1.

Results

Spatially variant optics in Eristalis

Hoverflies of the species under study here, *Eristalis tenax*, exhibit a sexual dimorphism of the eyes different from that of *Calliphora megacephala*. Male *Eristalis* have a fronto-dorsal region of large facet lenses, but despite the large facets, the distribution of interommatidial angles is similar to that of

females, with highest density near the frontal equator (Fig. 1). Thus, the large facets of male *Eristalis* create a 'bright zone' where light capture is increased but angular sensitivity is not specifically enhanced. Bright zones were first described in the blowfly *Chrysomyia megacephala* (van Hateren et al., 1989), which shares additional specializations found in *Musca*, such as a central rhabdomere (R7/R8) that contributes to lamina monopolar cells (LMCs) with the same absolute and spectral sensitivity as R1–6 (Franceschini et al., 1981; Hardie, 1983; Hardie et al., 1981). Although little is known about the behavior of *Chrysomyia*, the bright zone is suggested to serve a detect-and-track role. This also seems the most likely explanation for *Eristalis*. In the case of *Eristalis*, however, a detailed behavioral analysis (Collett and Land, 1978) shows that males track females in a manner similar to *Calliphora* and are also capable of a feat not observed in other flies – computation of an open-loop intercept course upon first seeing a target.

Local preferred directions in Eristalis

Fig. 2 shows the local preferred direction (LPD) and local motion sensitivity (LMS) for HS cells in *Eristalis*. Within the area of the receptive field we investigated, the distribution of LPDs and LMSs are similar to those of *Calliphora* HS cells, with a horizontally extended streak of large LMS to front-to-back ipsilateral motion. In this study, we encountered two classes of HS cells with dorsal receptive fields, one with maximal LMS at elevations between +30° and +60° (above the equator), and the other with maximal LMS near +30°. The neuroanatomy and receptive field properties of HS neurons in *Eristalis* are less well described than those of the blowfly, but our earlier work on these cells in female *E. tenax* highlights several likely similarities and differences (O'Carroll et al., 1997). Although nothing has yet been published for the equivalent organization of HS neurons in male flies of either species, the physiological location of these receptive fields corresponds to the anatomical locations of the dendritic arborizations of the female cells (O'Carroll et al., 1997). While further work is clearly required to describe and classify receptive field properties and neuroanatomy of these dorsal HS cells, we adopt here a classification for these two classes consistent with the blowfly and female *E. tenax* data. Hence we classify the more dorsal neurons as HSN (N: north) and the less northern neurons as HSNE (NE: north-equatorial). The frontal portion of the large receptive field of HSNE and, particularly, HSN cells in male *Eristalis* corresponds in location to the bright zone described above. The most sensitive region of the receptive field of *Eristalis* HSN is more dorsal than the *Calliphora* HSN, which more closely resembles the *Eristalis* HSNE in receptive field location (Hausen, 1982; Krapp et al., 2001).

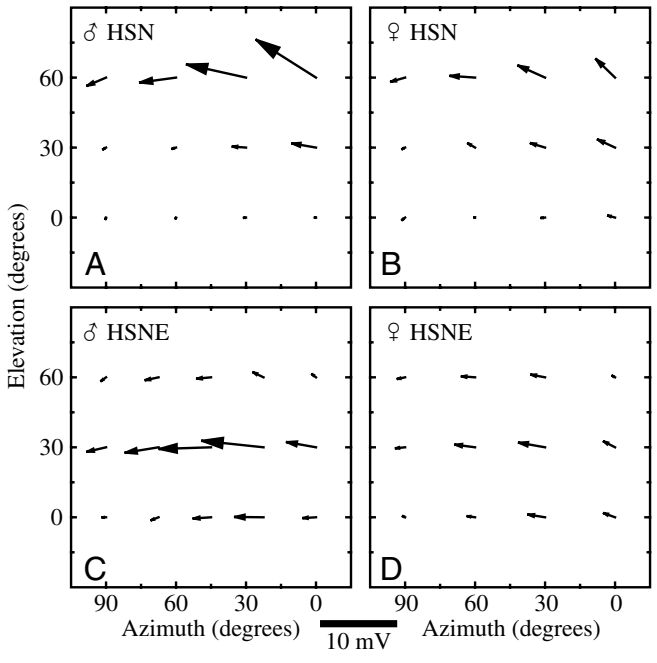

Fig. 2. Local preferred directions (LPD) and local motion sensitivities (LMS) of *Eristalis* LPTCs. The direction of the arrow indicates the LPD and the magnitude gives the LMS, as defined in the Materials and methods. The origin of the arrows is displayed on a Mercator projection, but the direction and magnitude are displayed using Euclidian geometry to facilitate LMS comparison (male HSN, *N*=3; female HSN, *N*=5; male HSNE, *N*=3; female HSNE, *N*=5). HSN, HSNE, horizontally sensitive N, NE neurones.

The stimulus employed to measure the LPD and LMS values is theoretically subject to the effects of motion adaptation as described in the methods. However, curves measured with the stimulus motion direction rotating in a clockwise manner were similar to those obtained from a counter-clockwise rotation. The median difference in clockwise and counter-clockwise measured LPDs across all locations, animals, sexes and cell types was 22°. The differences in LMS values were also quite small. The direction of LPD change was consistently opposite to the direction of the stimulus stepwise rotation, indicating that motion adaptation is responsible for the small shift in LPDs. Because the gain control component of motion adaptation is insensitive to the direction of the adapting stimulus (Harris et al., 2000), this effect is presumably due to a motion induced afterhyperpolarization-like effect.

In summary, the local preferred directions and local motion sensitivities resemble those of *Calliphora* measured at equivalent positions. This similarity suggests data from *Eristalis* HS cells may be suitable for exploring the matched filter hypothesis. Because LMS measured here and in earlier studies is not a predictor of the local velocity response characteristics (Krapp et al., 2001), an accurate prediction of local correlator output can only be made with accurate estimates of other local properties. In particular, the contrast–response relationship and its dependence on spatial and temporal frequency is required.

Response as a function of contrast

After determining the LPD and LMS of HS cells, small patches were selected from the large receptive field for further

detailed analysis. Because the distribution of LPDs and LMSs is so regular from fly to fly, we chose a stereotyped frontal and lateral location used in all experiments to test local properties. Sinusoidal gratings were localized to this region by multiplication with a Gaussian contrast window (i.e. a Gabor patch) with s.d.=7.1° and motion was always presented in the LPD as measured above. For HSN cells, the frontal location was centered at an azimuth and elevation of 0°, 60° with motion to 150° (up and left). The lateral location was at an azimuth and elevation of 90°, 60° with motion to 207° (down and left). For HSNE cells, the frontal location was centered at an azimuth and elevation of 0°, 30° with motion to 180° (leftward). The lateral location was at an azimuth and elevation of 90°, 30° with motion also to 180°.

The contrast–response relationship of these neurons in small patches was investigated using two alternative techniques (see Materials and methods). The first is a traditional contrast step technique in which contrast is stepped to a fixed value while membrane potential is recorded, as shown in Fig. 3A. This method suffers from two experimental difficulties. First, as described in the methods, selecting a time period for analysis is problematic because of the competing effects of onset transients and motion adaptation. For example, the response shown to contrast 0.215 appears to adapt rapidly. Second, the time required to perform a series of such experiments is prohibitive for intracellular recordings when trying to measure the contrast–response at a wide range of spatial and temporal frequencies. To overcome the problems of the contrast step, we used a contrast ramp method. Fig. 3B illustrates the time course of stimulus and response. Fig. 3C compares the results from the contrast step experiment of Fig. 3A with the contrast ramp experiment of Fig. 3B along with an analytic curve (Weibull function) used to fit the contrast ramp data. As can be seen, these two methods produce similar results, and the analytic curve fit to the contrast ramp data accurately captures the contrast–response relation measured with either method.

To determine if the contrast ramp method consistently replicates the contrast step method and to determine the goodness-of-fit of the analytic function, experiments of the type shown in Fig. 3C were repeated with varying parameters in several cells. Fig. 4 shows that, for several *Eristalis* HS cells under varying stimulus conditions, the contrast–response relation measured using the contrast ramp method (and an associated fit using an analytic function) is similar to the relation found when measured with the contrast step method. Because it is much faster at measuring the contrast–response relationship, we used the contrast ramp as the primary stimulus with which to measure spatio-temporal contrast sensitivity.

Spatio-temporal surfaces

Fig. 5 shows the mean responses of a male HSN cell to multiple presentations of a contrast ramp stimulus of varying spatial and temporal frequency plotted on a logarithmic contrast axis. The stimulus was presented in the frontal location. The analytic fits (shown in red) differ only slightly from the data where there is little noise. Where there is substantial noise, the automatic fits appear similar to the best possible 'by eye', suggesting that the analytic fits can be used to accurately estimate the response of these cells.

To view the resultant data plotted against spatial and/or temporal frequency axes, it is necessary to reduce the dimensionality of the data from an entire contrast–response relationship at any given combination of spatial and temporal frequency. We therefore used the analytic fit data to compute estimated response at a contrast of 1.0 (high contrast regime), estimated response at a contrast of 0.2 (low contrast regime), and the contrast sensitivity, or reciprocal of the threshold contrast, required to reach a criterion response of 2 mV. Note that contrast sensitivity, the reciprocal of threshold contrast, is a unitless value like contrast itself.

To visualize this spatio-temporal data, it is convenient to construct a contour plot showing the response estimated using the analytic fits. Fig. 6A,B shows the estimated response surface in the high-contrast regime for the frontal and lateral portions of the receptive field of the male HSN neuron in Fig. 5. The results from this cell are similar to those of other cells; responses to lateral stimuli were consistently weaker than responses to frontal stimuli

The velocity of sinusoidal grating stimuli is the ratio of temporal frequency to spatial frequency. Lines of iso-velocity therefore have an approximate lower-left to upper-right direction in these spatio-temporal surface plots. The 'preferred velocity' is defined by the ratio of temporal to spatial frequency that elicits maximal response, and thus passes through the peaks on the spatio-temporal surface. An iso-velocity line at this preferred velocity, and thus through the peak of the spatio-temporal tuning surfaces, is drawn in each panel of Fig. 6. In this neuron and consistent with our other results, the preferred velocity frontally is faster than that laterally, mainly due to faster temporal frequency tuning as seen by shift of the peak to faster temporal frequencies in the frontal field compared to the lateral field.

Evident in the contour plot of Fig. 6B, and to a lesser degree in Fig. 6A, is a diagonally orientated 'ridgeline', which appears to run from northeast to southwest. This diagonal orientation appears in the response and contrast sensitivity data indicates that the responses of these cells are not completely separable in space and time. In fact, the dominant orientation appears to be in the iso-velocity direction, and these cells therefore exhibit a degree of tuning directly for grating velocity rather than purely temporal and spatial frequency. Such 'speed tuning' can be obtained from a correlator model with imperfectly balanced subunit subtraction (Egelhaaf et al., 1989; Zanker et al., 1999). The 'VT' descending neurons of the honeybee exhibit a much larger degree of velocity tuning when tested with sinusoids and may be involved in flight speed control (Ibbotson, 2001).

Regional and sex-specific variation in spatio-temporal properties

We compared response amplitude, contrast sensitivity, and tuning to temporal and spatial frequencies across receptive field

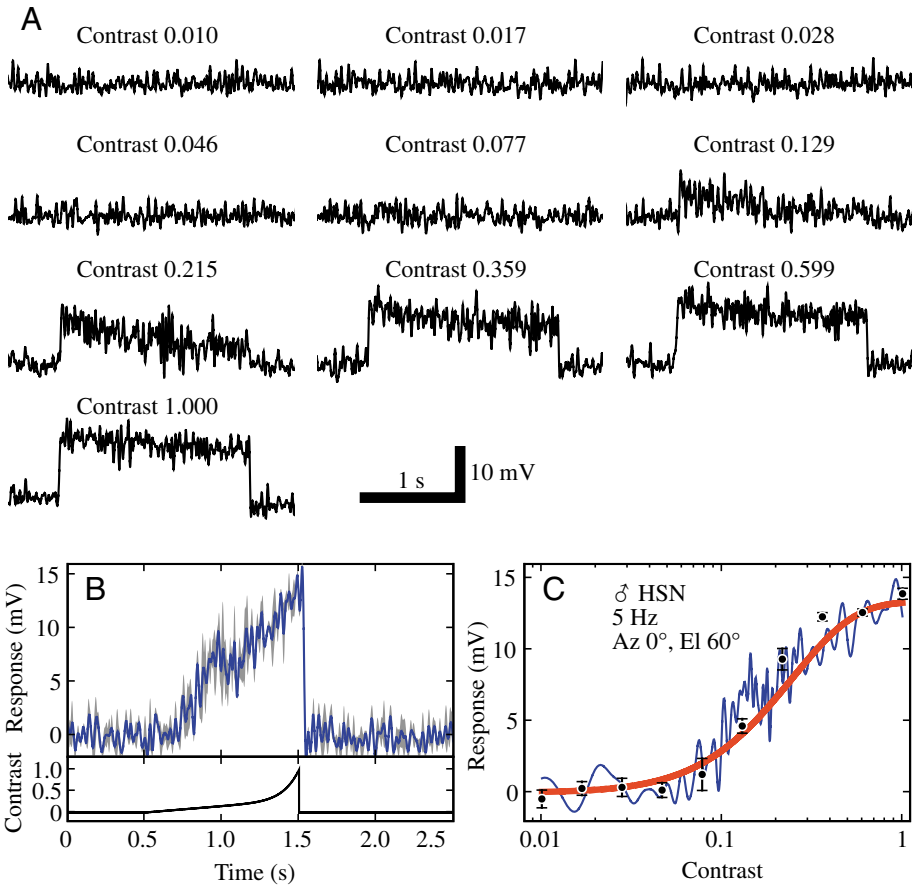

Fig. 3. Response as a function of contrast of Gaussian windowed sinusoidal grating (Gabor patch). (A) Single trials showing responses to traditional 'contrast step' stimulus. (B) 'Contrast ramp' stimulus measures contrast–response relationship more rapidly. Blue line shows mean response and gray fill shows mean response ± instantaneous s.d. (C) Comparison of methods shown in A and B plotted on logarithmic contrast axis. Smooth red line shows analytic fit to contrast ramp data. Data are from frontal portion of the receptive field of a single male HSN cell viewing sinusoidal grating at 0.1 cycles deg.$^{-1}$ at 5 Hz. Values are means ± s.d. from at least 3 trials. Az, azimuth; El, elevation.

locations and sexes. To facilitate these comparisons, slices were taken across spatio-temporal surfaces resulting in spatial and temporal frequency tuning curves. The response amplitudes and contrast sensitivity of HSN cells to a variety of temporal (Fig. 7) and spatial frequencies (Fig. 8) indicate that the most pronounced difference between frontal and lateral parts of the receptive field is a substantially increased gain and sensitivity to frontal stimuli, particularly in males, in which this

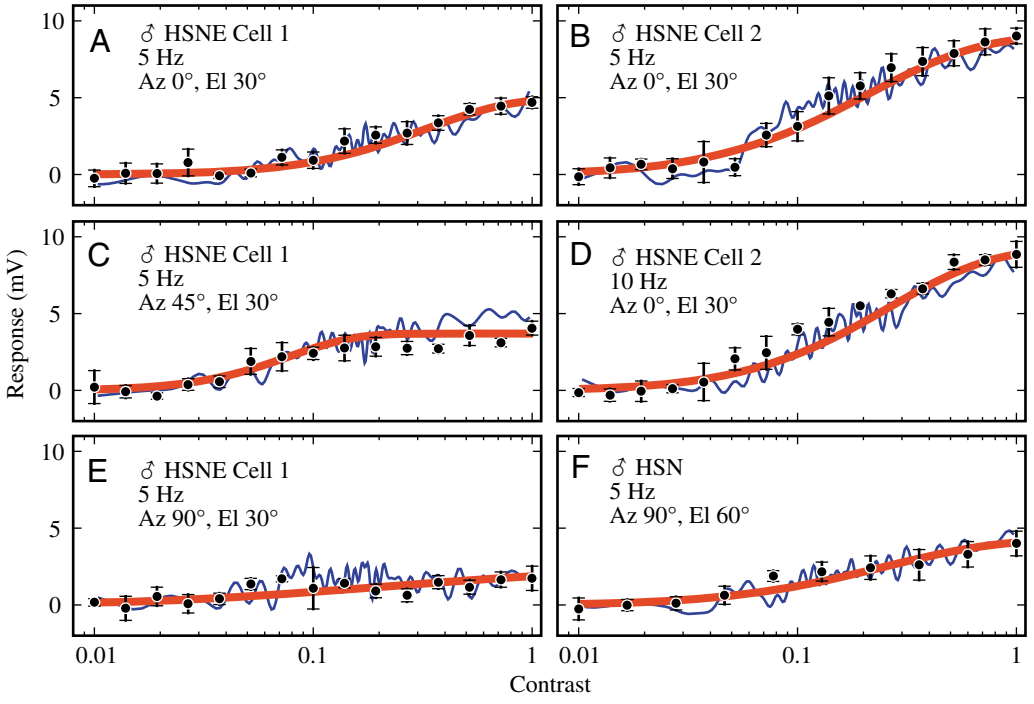

Fig. 4. Summary of contrast–response relation under several conditions showing that the contrast ramp method estimates contrast sensitivity similarly to the contrast step method, but much more quickly. Data analyzed as in Fig. 3C. All parameters as listed, spatial frequency= 0.1 cycles deg.$^{-1}$. (A–E) Data from two HSNE cells from several retinal locations. (F) HSN cell from Fig. 3 viewing laterally positioned grating. All data from male flies. Values are means ± instantaneous s.d. from a minimum of 3 trials. Az, azimuth; El, elevation.

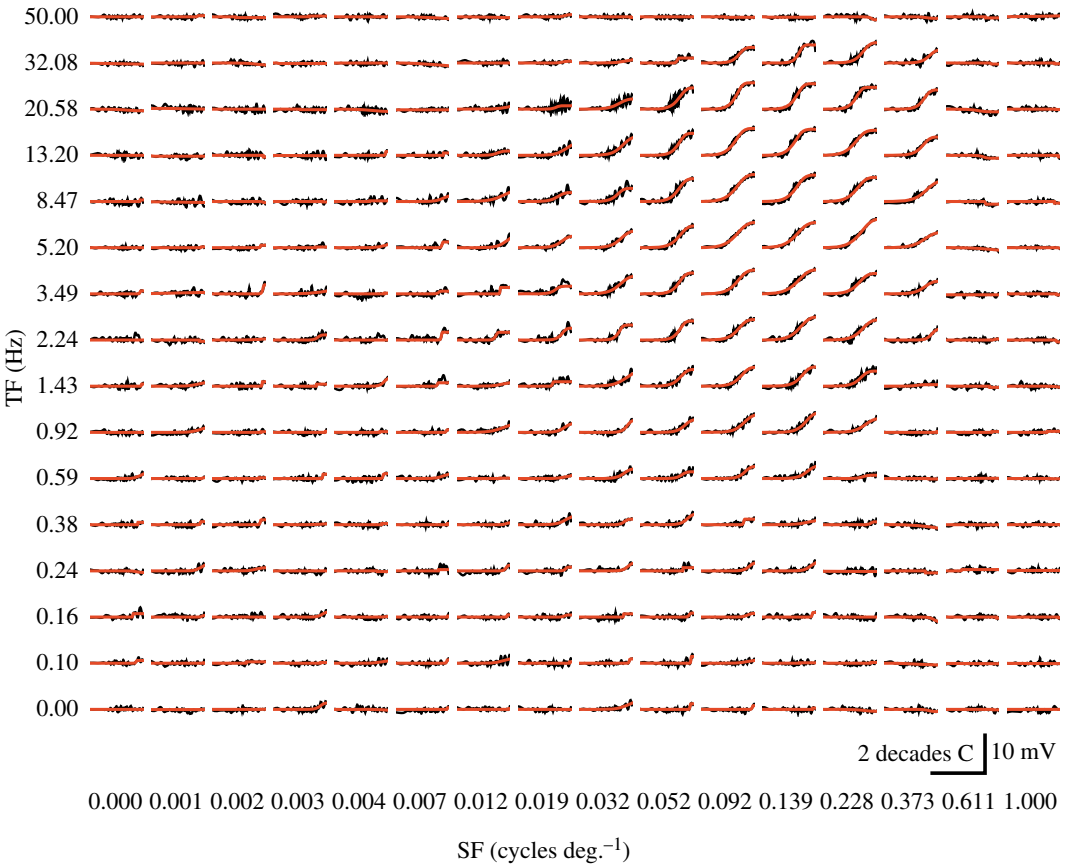

Fig. 5. Responses to contrast ramp stimulus at a range of temporal (TF) and spatial frequencies (SF) in the frontal portion of the receptive field of a single male HSN neuron. The mean response to 3 or more trials is shown in black for each combination of spatial and temporal frequency as plotted as in Fig. 3C. Parameter fits are shown in red. The data are plotted on logarithmic contrast axis. Minimum of 3 trials per trace; azimuth=0°, elevation=60°. Details of fitting described in Materials and methods. Decade C, tenfold Michelson contrast variation.

region of the receptive field is associated with the optical bright zone. Maximal contrast sensitivity in males in this region is 12.9 (Fig. 7E), and in females it is 8.6 (Fig. 8E). Laterally, these values fall to 8.1 and 3.5 in males and females, respectively (Fig. 8F). HSNE (Figs 9, 10) cells show a similar trend, although the magnitude of the differences is less.

In HSN cells, there is also a large sexual dimorphism in the temporal frequency domain. The frontal portion of the male HSN receptive field is tuned to faster stimuli than that of females, with the optimum near 13 Hz in males and 3.5 Hz in females in both the high-and low-contrast regimes (Fig. 7A,C). In the lateral portions of the receptive field, the situation is similar, although the optima are slower at 3.5 Hz in males and 1.4 Hz in females (Fig. 7B,D). HSNE cells (Fig. 9) have much less pronounced temporal frequency tuning differences between the sexes. The frontal to lateral variation is similar to the HSN data. Male *Eristalis* HS cells were known to have faster temporal frequency

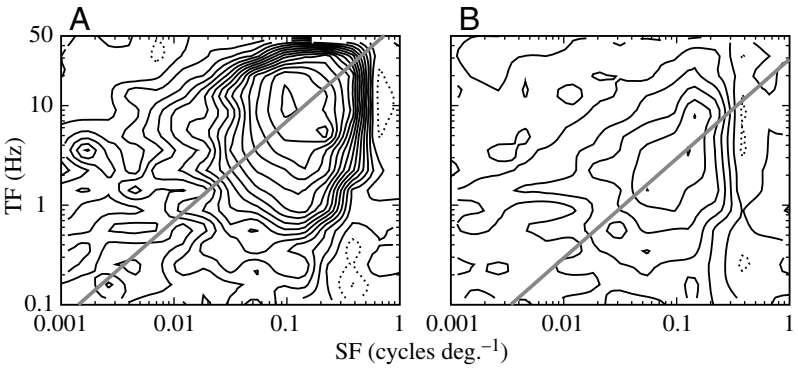

Fig. 6. Contrast–response surfaces of a single male HSN cell showing faster temporal dynamics and higher spatial frequency tuning in the frontal portion of the receptive field. The thick gray line in each panel is an iso-velocity line at the preferred velocity, the optimal temporal frequency (TF) divided by the optimal spatial frequency (SF). (A) Data are from the frontal portion of the receptive field, azimuth=0°, elevation=60°. (B) Data are from the lateral portion of the receptive field, azimuth=90°, elevation=60°. Height of surface is the estimated response to a grating of Michelson contrast 1.0 based on fit parameters calculated at each spatial and temporal frequency. Fit parameters for A are shown in Fig. 5. Contour interval=1.0 mV, with negative responses dotted.

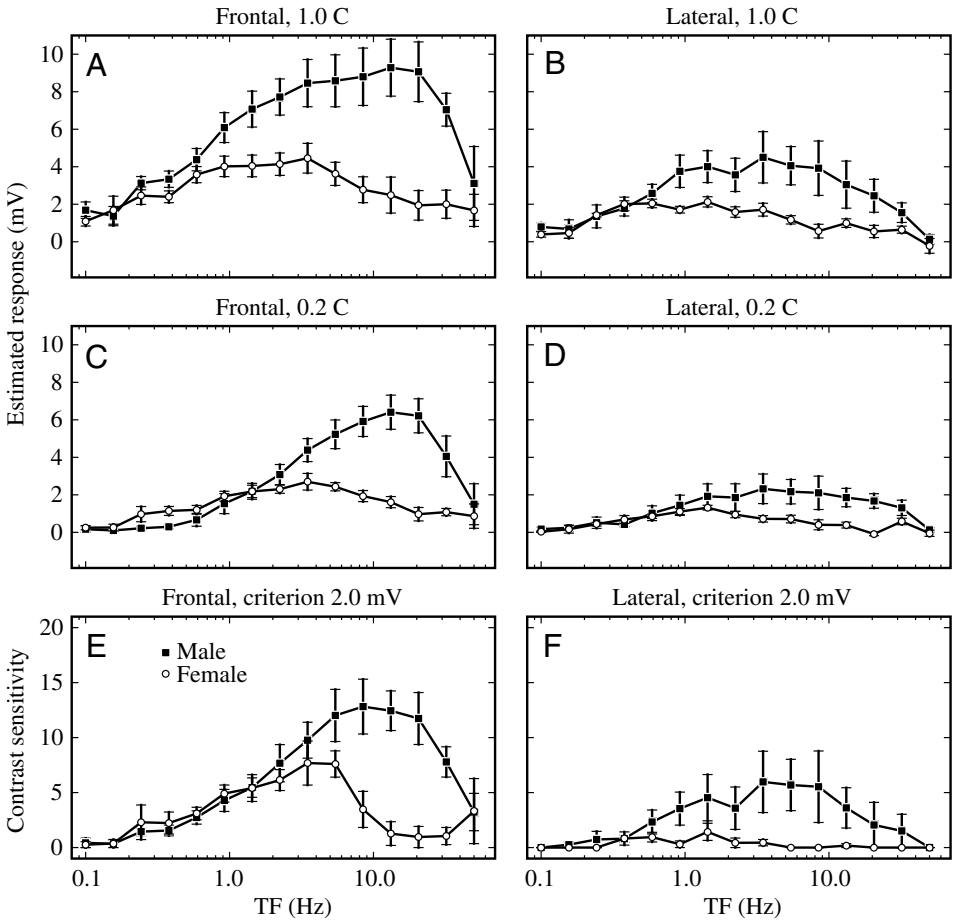

Fig. 7. Comparison of temporal frequency (TF) tuning at two receptive field locations of HSN cells showing sexually dimorphic contrast sensitivity and temporal dynamics. Frontal receptive field (A,C,E) for HSN cells is defined as 0° azimuth and 60° elevation. Lateral receptive field (B,D,F) is defined as 90° azimuth and 60° elevation. Responses were estimated for Michelson contrasts 1.0 (A,B) and 0.2 (C,D) and the contrast sensitivity was calculated for a criterion response of 2 mV (E,F). Estimated response and contrast sensitivity were calculated from contrast ramp data (for details see Materials and methods). Spatial frequency 0.1 cycles deg.$^{-1}$. Values are means ± s.e.m.; males, *N*=5 (filled squares), females, *N*=6 (open circles).

tuning than females (O'Carroll et al., 1997), and this study shows that this sex difference is largely confined to HSN cells.

Fig. 8 shows the spatial frequency tuning of male (filled squares) and female (open circles) *Eristalis* HSN cells measured frontally and laterally. Also shown are model motion detector responses that estimate the contribution of Type 1 and Type 2 EMDs based on the interommatidial angle taken from Fig. 1 and some limited assumptions about spatial processing (see Materials and methods). The model parameters that provide a best fit to the data are shown in Table 1 and are illustrated in graphical form as insets in Fig. 8. Other than contrast sensitivity and gain changes, the curves show only subtle differences in spatial frequency tuning between frontal and lateral portions of the receptive field and between males and females. Similar observations for HSNE cells apply (Fig. 10).

Because temporal frequency tuning curves measured frontally show stronger responses to fast stimuli than those measured laterally and because the spatial frequency tuning curves have significantly less regional variation, the 'preferred velocities' of the frontal regions of HSN and HSNE neurons are predicted to be faster than laterally. This is true for both sexes but is most evident in the male HSN neuron.

The model motion detector responses provide a good fit to the experimentally measured data. Type 1 EMDs appear to dominate the response of both HSN and HSNE cells (Table 1). This agrees with previous experimental work on other flies in light-adapted conditions (Buchner, 1984; Srinivasan and Dvorak, 1980). The amount of saturation in the model can be inferred from the flatness of the curve, and the overall gain can be inferred by the height of the curve. The effects of saturation can be seen as a broad, flat peak, particularly in the high contrast male data (Fig. 8A, Fig. 10A). This saturation necessitated a saturating component in the model motion detector used to fit the responses. Model responses descend below zero at some high spatial frequencies, a prediction of 'spatial aliasing', which is sometimes observed in *Eristalis* cells when stimulating with local grating patches (e.g. Fig. 6A,B). The amount of spatial aliasing predicted is greater than observed. Because the model used does not explicitly sum the outputs of two correlators to produce the Type 1 EMD output but only uses a single correlator with short baseline, the amount of aliasing is overestimated (van Hateren, 1990). With a larger optical acceptance angle $\Delta\rho$, spatial aliasing would be attenuated because of greater low-pass filtering, and adjusting the ratio of $\Delta\rho$ to $\Delta\phi$ from the value of 1.0 used here varied the magnitude of predicted spatial aliasing but had little effect on the estimated contributions of Type 1 and Type 2 EMDs (not shown). Therefore, this difference is not expected to have any significant effect on the conclusion that motion detection

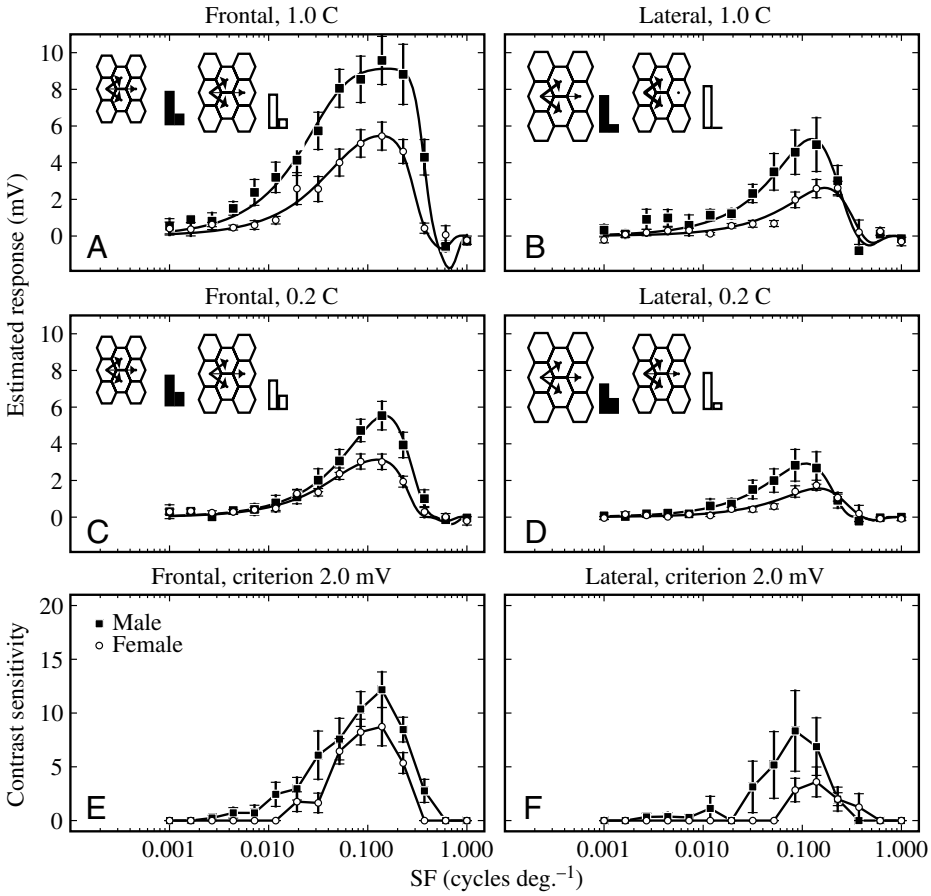

Fig. 8. Comparison of spatial frequency (SF) tuning at two receptive field locations of HSN cells showing sexually dimorphic contrast sensitivity and lateral spatial frequency tuning. Estimated contributions from Type 1 and Type 2 EMDs are given as arrow thickness and again as the height of small bars. EMD contributions and smooth curves were fit to the shown data with a two EMD model constrained by interommatidial angle data taken from Fig. 1. Free parameters were total gain, relative EMD contribution, and saturation. These parameters can be found in Table 1. Temporal frequency 5 Hz. Values are means ± s.e.m.; males, *N*=5 (filled squares), females, *N*=6 (open circles).

Table 1. *Motion detector model parameters used to fit spatial frequency tuning data*

			$\Delta\phi$[a] (deg.)	g_1	g_2	k	s	$F_{s,opt}$[b] (cycles deg.$^{-1}$)
High contrast regime								
Female	HSN	Frontal	1.4	0.80	0.20	6.32	1.73	0.14
		Lateral	1.4	1.00	0.00	122.86	0.03	0.17
	HSNE	Frontal	1.15	0.69	0.31	4.58	2.27	0.15
		Lateral	1.4	1.00	0.00	207.14	0.01	0.17
Male	HSN	Frontal	1.2	0.77	0.23	9.25	3.30	0.16
		Lateral	1.6	0.85	0.15	228.43	0.03	0.12
	HSNE	Frontal	1.075	0.82	0.18	5.91	3.09	0.18
		Lateral	1.38	1.00	0.00	44.58	0.10	0.17
Low contrast regime								
Female	HSN	Frontal	1.4	0.68	0.32	4.09	1.32	0.12
		Lateral	1.4	0.86	0.14	28.83	0.07	0.14
	HSNE	Frontal	1.15	0.57	0.43	3.19	1.61	0.14
		Lateral	1.4	0.83	0.17	102.38	0.02	0.14
Male	HSN	Frontal	1.2	0.71	0.29	16.32	0.46	0.15
		Lateral	1.6	0.68	0.32	11.18	0.35	0.11
	HSNE	Frontal	1.075	0.83	0.17	5.17	1.27	0.18
		Lateral	1.38	0.76	0.24	74.49	0.04	0.13

For explanation of parameters, see Materials and methods.
[a]Taken from Fig. 1.
[b]Calculated from the other parameters listed.

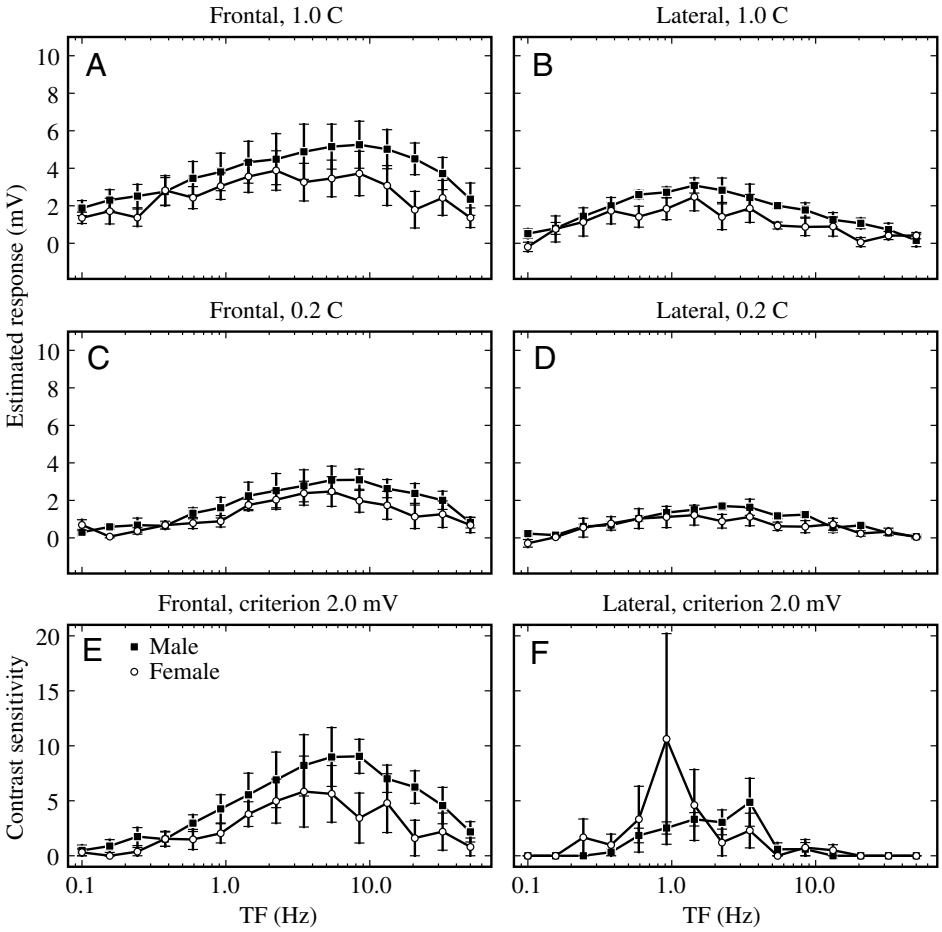

Fig. 9. Comparison of temporal frequency (TF) tuning at two receptive field locations of HSNE cells showing little sexually dimorphic contrast sensitivity or temporal dynamics. Spatial frequency 0.1 cycles deg.$^{-1}$. Values are means ± s.e.m.; males, *N*=4 (filled squares), females, *N*=5 (open circles).

is dominated by Type 1 (nearest neighbor) EMDs in light-adapted *Eristalis* HSN cells.

Discussion

To summarize our results, Male *Eristalis* have an optical 'bright zone' in the fronto-dorsal eye, where larger facets result in increased light capture compared to females. In contrast to results seen in other large flies where the region of largest facet diameter and minimum interommatidial angle coincide, the region of maximal spatial resolution in male *Eristalis* is equatorial, although a large region of increased spatial resolution does extend into the dorsal-frontal region. Correspondingly, the large receptive fields of the motion detecting HS neurons are inhomogeneous across space. Regional and sexually dimorphic differences exist in spatial tuning, temporal tuning and contrast sensitivity. The pattern of local contrast sensitivity and response amplitude is predicted by the optical variation in facet diameter; local stimulation of portions of the receptive field served by large diameter facet lenses, particularly in the bright zone of males, produces responses stronger than the same stimuli presented laterally. Temporal frequency tuning is also substantially faster in this frontal portion of the world, indicating that there is also sexual dimorphism in the dynamics of HSN cells. The lack of such dramatic sexually dimorphic temporal frequency tuning in HSNE neurons emphasizes the localized nature of the sex-specific properties. Variations in spatial frequency tuning are predicted by a model using experimentally determined optical parameters and dominated by contributions from Type 1 EMDs, indicating that sex-specific differences are limited primarily to the optics. All of these sex-specific differences indicate that the bright zone plays an important role in affecting the local properties of motion detectors.

Contrast sensitivity

The relationship between contrast and response is important to the function of these cells because it is strongly non-linear and plays an important role determining response characteristics (Dror et al., 2001; Egelhaaf et al., 1989; Shoemaker et al., 2001). By measuring the contrast–response relationship rather than responses to a particular contrast, this study was able to characterize responses in both low- and high-response regimes. The low-response regime is important because in this regime of small signal amplitudes, the system is most linear, and can be used, for example, to investigate essential properties of motion detection without additional non-linearities such as saturation (Reichardt et al., 1983) or adaptation (de Ruyter van Steveninck et al., 1986; Harris et al., 2000; Maddess and Laughlin, 1985). The high-response regime

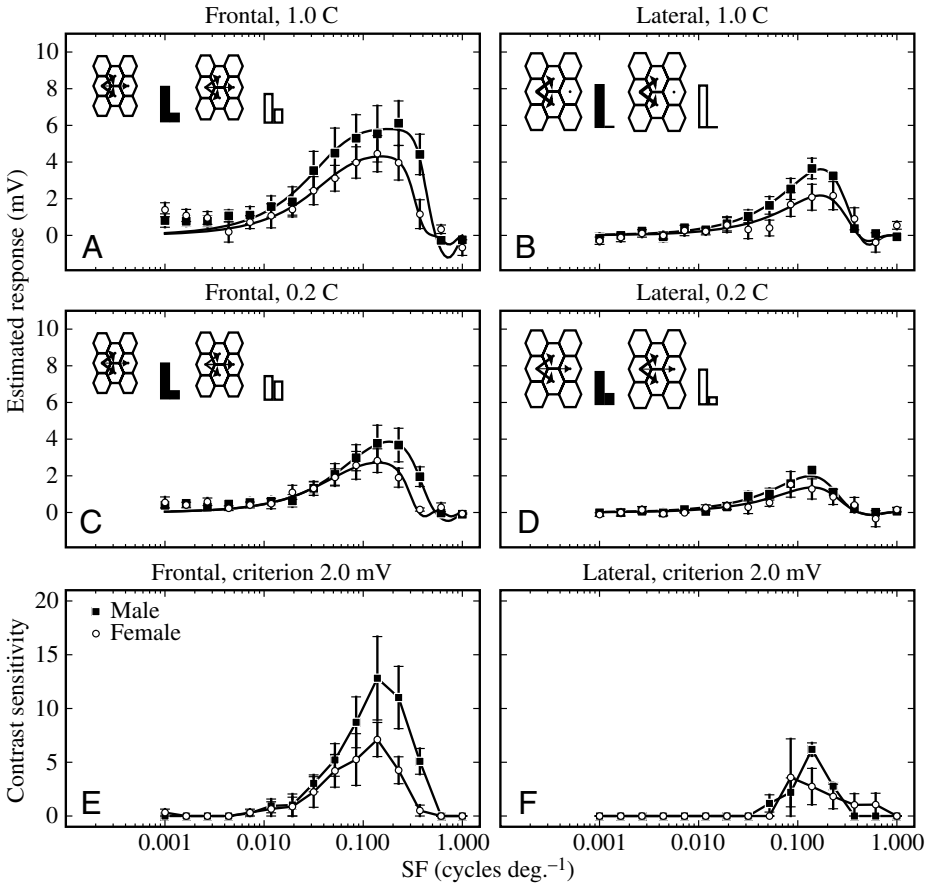

Fig. 10. Comparison of spatial frequency tuning at two receptive field locations of HSNE cells showing little sexually dimorphic contrast sensitivity and lateral spatial frequency tuning. Temporal frequency 5 Hz. Values are means ± s.e.m.; males, *N*=4 (filled squares), females, *N*=5 (open circles).

is presumably behaviorally relevant but is difficult to interpret, at least in restrained animals where electrophysiology has typically been performed. This may be due to additional non-linearities such as saturation. One example from the fly *Bombylius* suggests that saturation due to high contrast into to fly LPTCs leads to broad tuning curves, masking the underlying contribution from multiple input channels (O'Carroll, 2001).

Matched filter hypothesis

As discussed in the introduction, the local preferred directions (LPDs) of lobula plate tangential cells (LPTCs) appear to match the pattern of optic flow induced by self motion. Over the regions our stimulus device allowed us to test, we found that in *Eristalis* HS cells, local preferred directions (LPDs) are similar to those of *Calliphora* HS cells. (See Results for a more detailed comparison of LPDs between *Eristalis* and *Calliphora*.) Our results in *Eristalis* appear inconsistent with the suggestion that HS cells may function as matched filters for yaw rotation in *Calliphora* (Krapp et al., 2001). The *Eristalis* HS cells studied have faster preferred velocities frontally rather than laterally at the same elevation angle; yaw rotation produces motion of constant velocity both frontally and laterally. We note, however, that a more detailed interpretation of HS receptive fields in *Calliphora*, including the effects of contralateral input, suggests a possible role in translation detection (Krapp, 2000). In the present study, we found no evidence of contralateral input to the *Eristalis* HS cells. As discussed below, this is particularly evident in males and could be the result of conflicting demands that target detection circuitry imposes on upstream processing elements of the visual system and results in compromised performance of *Eristalis* HS cells in estimating yaw rotation. The general trend, however, was also found in females and it may be some *Eristalis*-specific phenomenon. Alternatively, the faster temporal frequency tuning in frontally directed EMDs could be a more general phenomenon not yet observed in other fly species.

Prediction of responses to naturalistic, global optic flow is not simply a linear summation of LPD and LMS values. One needs to take into account local variation of spatial, temporal and contrast sensitivity and how these local response properties are integrated spatially and temporally into membrane potential at the output regions of the neuron. The large regional differences in contrast sensitivity and temporal frequency tuning we found, in HSN for example, are not particularly evident in the map of LPD/LMS, and thus highlight the difficulty of predicting responses based solely on this characterization. Indeed, one study (Karmeier et al., 2003) shows that the responses of the V1 cell, a spiking LPTC predicted to be sensitive to pitch-like optic flow, responds strongly to any global motion with a strong frontal downward component (although the preferred rotation axis stays unchanged even if lift translation is combined with rotation).

An alternative, but not mutually exclusive, view of LPTC encoding of self motion has recently been proposed, which suggests that HS may encode both rotational and translational information in different frequency bands, although the means flies might use to decode this information is unclear (Kern et al., 2005). Nevertheless, some wide-field properties are well predicted from LPDs and LMSs, such as the preferred rotation axes of VS neurons (Karmeier et al., 2005).

The bright zone: sex-specific specialization for target detection?

The high contrast sensitivity and fast temporal frequency tuning directed fronto-dorsally in male *Eristalis* HSN cells coincides with a sex-specific region of large diameter facet lenses. In most other insects, including flies, large lenses are associated with fine angular resolution, but in this case, male interommatidial angles across the eye are similar to those of the female, being most closely spaced near the equator. Thus male photoreceptors in the 'bright zone' capture more light than photoreceptors elsewhere, such as in the male blowfly *Chrysomyia megacephala* (van Hateren et al., 1989). The enhanced contrast sensitivity of the portion of the receptive field directed toward this region indicates that higher retinal illuminance made available by the optics is utilized by the motion detection system.

The suggestion that light capture is at a premium in the fronto-dorsal region of male *Eristalis* eyes leads to the question of sex-specific behavior. Within 100 ms of seeing a moving object, male *Eristalis* compute and initiate an intercept course based on the position and velocity of the moving target in addition to some 'hardwired' biological constants such as the size and speed of conspecific females (Collett and Land, 1978). This interception behavior of *Eristalis* (and *Volucella*) is fundamentally different from the tracking behavior of other flies in that it requires that the initial flight is directed away from the retinal image of the target. If the target was indeed a conspecific female and the initial open-loop interception behavior was successful, it would be followed by closed-loop tracking similar to that found in other flies (Land and Collett, 1974). Although different in computation (computing an intercept course requires turning away from a target while the reverse is true for tracking), both of these visually guided behaviors distinguish males from females and presumably push the visual system to its limit. This sex-specific behavior is hypothesized to have driven the evolution of sex-specific specializations at the optical and neural levels.

Although evidence regarding regionally specific properties of motion detection comes from HSNE and particularly HSN cells in the present study, it is unknown whether these cells are directly involved with target detection or tracking behaviors. Large stimuli are required to produce maximal responses in these HS cells, and the retinal image of another fly at distances greater than a few millimeters would be substantially smaller than even the small stimuli used in this study. In male *Eristalis*, a class of small-target motion detecting (STMD) neurons in the lobula selectively responds to small objects (Nordstrom et al., 2006). Despite being tuned to respond preferentially to very small objects, these STMDs share a similar fronto-dorsal receptive field (within the 'bright zone') with HSN. One possibility is that a single common set of elementary motion detectors (EMDs) may serve as upstream input to the dual tasks of target and wide field motion detection. In this fronto-dorsal region of the visual world, these computational tasks may place conflicting demands on the temporal tuning of the elementary motion detectors; *Eristalis* HS cells are suggested to stabilize hovering, a task requiring sensitivity to low velocities and observed in both sexes when feeding and maneuvering, but the fast temporal tuning in males indicates alternate demands (O'Carroll et al., 1997). An increase of contrast sensitivity would be beneficial to both low-velocity detection and small target detection and may increase performance of the compromise solution to acceptable levels for both tasks. In other words, although we believe HS cells are involved in course control and hovering stabilization in both sexes, our results suggest that in males, EMDs upstream from the HSN neuron, in particular, may be subjected to conflicting demands imposed by target tracking behaviors. Fast motion detectors require fast input signals, which must come from fast photoreceptors. Fast fly photoreceptors are energetically expensive (Laughlin et al., 1998) and have lower signal-to-noise ratios (Laughlin, 1994). The above arguments suggest that fast, highly contrast-sensitive motion detection in male *Eristalis* is an expensive adaptation in terms of optics (large facets), photoreceptor energy expenditure, and possibly the ability to detect low speeds useful for stabilizing hovering.

List of abbreviations and symbols

A	amplitude
d	dorsal
D	facet diameter
EMD	elementary motion detector
f	frontal
F_s	spatial frequency
g_1	model Type 1 EMD gain term
g_2	model Type 2 EMD gain term
HS	'Horizontal System' cell
k	model gain term
l	lateral
LMS	local motion sensitivity
LPD	local preferred direction
LPTC	lobula plate tangential cell
MTF	modulation transfer function
s	model saturation term
SF	spatial frequency
t	time
TF	temporal frequency
VS	'Vertical System' cell
$\Delta\phi$	interommatidial angle
$\Delta\rho$	acceptance angle
θ	local motion angle

This work was supported through a Predoctoral Fellowship from the Howard Hughes Medical Institute to A.D.S. and grants from the United States Air Force Office of Scientific Research/Asian Office for Aerospace Research and Development (FA9550-04-1-0294). We thank the Botanical Gardens of Adelaide for allowing us to collect *Eristalis*, Sara Juhl for performing the optical measurements, Dr Gaby Maimon for careful reading and discussion of the manuscript, and an anonymous reviewer for detailed, helpful comments.

References

Boeddeker, N., Kern, R. and Egelhaaf, M. (2003). Chasing a dummy target: smooth pursuit and velocity control in male blowflies. *Proc. R. Soc. Lond. B Biol. Sci.* **270**, 393-399.

Boeddeker, N., Lindemann, J. P., Egelhaaf, M. and Zeil, J. (2005). Responses of blowfly motion-sensitive neurons to reconstructed optic flow along outdoor flight paths. *J. Comp. Physiol. A* **191**, 1143-1155.

Buchner, E. (1976). Elementary movement detectors in an insect visual-system. *Biol. Cybern.* **24**, 85-101.

Buchner, E. (1984). Behavioral analysis of spatial vision in insects. In *Photoreception and Vision in Invertebrates* (ed. M. A. Ali), pp. 561-621. New York: Plenum.

Bülthoff, H., Little, J. and Poggio, T. (1989). A parallel algorithm for real-time computation of optical flow. *Nature* **337**, 549-553.

Burton, B. G., Tatler, B. W. and Laughlin, S. B. (2001). Variations in photoreceptor response dynamics across the fly retina. *J. Neurophysiol.* **86**, 950-960.

Buschbeck, E. K. and Strausfeld, N. J. (1996). Visual motion-detection circuits in flies: small-field retinotopic elements responding to motion are evolutionarily conserved across taxa. *J. Neurosci.* **16**, 4563-4578.

Buschbeck, E. and Strausfeld, N. J. (1997). The relevance of neural architecture to visual performance: Phylogenetic conservation and variation in Dipteran visual systems. *J. Comp. Neurol.* **383**, 282-304.

Collett, T. S. and Land, M. F. (1978). How hoverflies compute interception courses. *J. Comp. Physiol. A* **125**, 191-204.

Dahmen, H., Franz, M. O. and Krapp, H. G. (2001). Extracting egomotion from optic flow: limits of accuracy and neural matched filters. In *Motion Vision – Computational, Neural, and Ecological Constraints* (ed. J. M. Zanker and J. Zeil), pp. 143-168. Berlin, Heidelberg, New York: Springer Verlag.

de Ruyter van Steveninck, R. and Laughlin, S. B. (1996). The rate of information transfer at graded-potential synapses. *Nature* **379**, 642-645.

de Ruyter van Steveninck, R. R., Zaagman, W. H. and Mastebroek, H. A. K. (1986). Adaptation of transient responses of a movement-sensitive neuron in the visual-system of the blowfly *Calliphora erythrocephala*. *Biol. Cybern.* **54**, 223-236.

Dror, R. O., O'Carroll, D. C. and Laughlin, S. B. (2001). Accuracy of velocity estimation by Reichardt correlators. *J. Opt. Soc. Am. A* **18**, 241-252.

Dvorak, D., Srinivasan, M. V. and French, A. S. (1980). The contrast sensitivity of fly movement-detecting neurons. *Vision Res.* **20**, 397-407.

Egelhaaf, M. and Borst, A. (1989). Transient and steady-state response properties of movement detectors. *J. Opt. Soc. Am. A* **6**, 116-127.

Egelhaaf, M. and Borst, A. (1993). Movement detection in arthropods. In *Visual Motion and its Role in the Stabilization of Gaze* (ed. F. A. Miles and J. Wallman). New York: Elsevier Science Publishers.

Egelhaaf, M., Borst, A. and Reichardt, W. (1989). Computational structure of a biological motion-detection system as revealed by local detector analysis in the fly's nervous-system. *J. Opt. Soc. Am. A* **6**, 1070-1087.

Franceschini, N. (1975). Sampling of visual environment by the compound eye of the fly: fundamentals and applications. In *Photoreceptor Optics* (ed. A. W. Snyder and R. Menzel), pp. 98-125. Berlin, Heidelberg, New York: Springer.

Franceschini, N., Hardie, R., Ribi, W. and Kirschfeld, K. (1981). Sexual dimorphism in a photoreceptor. *Nature* **291**, 241-244.

Franz, M. O. and Krapp, H. G. (2000). Wide-field, motion-sensitive neurons and matched filters for optic flow fields. *Biol. Cybern.* **83**, 185-197.

Franz, M. O., Chahl, J. S. and Krapp, H. G. (2004). Insect-inspired estimation of egomotion. *Neural Comput.* **16**, 2245-2260.

Götz, K. G. (1964). Optomotorische untersuchung des visuellen systems einiger augenmutanten der fruchtfliege *Drosophila*. *Kybernetik* **2**, 77-92.

Hardie, R. C. (1983). Projection and connectivity of sex specific photoreceptors in the compound eye of the male housefly (*Musca domestica*). *Cell Tissue Res.* **233**, 1-21.

Hardie, R. C., Franceschini, N., Ribi, W. and Kirschfeld, K. (1981). Distribution and properties of sex specific photoreceptors in the fly *Musca domestica*. *J. Comp. Physiol. A* **145**, 139-152.

Harris, R. A., O'Carroll, D. C. and Laughlin, S. B. (1999). Adaptation and the temporal delay filter of fly motion detectors. *Vision Res.* **39**, 2603-2613.

Harris, R. A., O'Carroll, D. C. and Laughlin, S. B. (2000). Contrast gain reduction in fly motion adaptation. *Neuron* **28**, 595-606.

Hausen, K. (1982). Motion sensitive interneurons in the optomotor system of the fly. II. The horizontal cells – receptive-field organization and response characteristics. *Biol. Cybern.* **46**, 67-79.

Hausen, K. and Strausfeld, N. J. (1980). Sexually dimorphic interneuron arrangements in the fly visual system. *Proc. R. Soc. Lond. B Biol. Sci.* **208**, 57-71.

Hooke, R. (1665). *Micrographia: Or Some Physiological Descriptions Of Minute Bodies Made By Magnifying Glasses.* London: John Martyn and James Allestry.

Hornstein, E. P., O'Carroll, D. C., Anderson, J. C. and Laughlin, S. B. (2000). Sexual dimorphism matches photoreceptor performance to behavioural requirements. *Proc. R. Soc. Lond. B Biol. Sci.* **267**, 2111-2117.

Ibbotson, M. R. (2001). Evidence for velocity tuned motion-sensitive descending neurons in the honeybee. *Proc. R. Soc. Lond. B Biol. Sci.* **268**, 2195-2201.

James, A. C. (1990). White-noise studies in the fly lamina. PhD thesis, Canberra, Australian National University, Australia.

Karmeier, K., Krapp, H. G. and Egelhaaf, M. (2003). Robustness of the tuning of fly visual interneurons to rotatory optic flow. *J. Neurophysiol.* **90**, 1626-1634.

Karmeier, K., Krapp, H. G. and Egelhaaf, M. (2005). Population coding of self-motion: applying Bayesian analysis to a population of visual interneurons in the fly. *J. Neurophysiol.* **94**, 2182-2194.

Kern, R., van Hateren, J. H., Michaelis, C., Lindemann, J. P. and Egelhaaf, M. (2005). Function of a fly motion-sensitive neuron matches eye movements during free flight. *PLoS Biol.* **3**, 1130-1138.

Kirschfeld, K. (1976). The resolution of lens and compound eyes. In *Neural Principles in Vision* (ed. F. Zettler and R. Weiler), pp. 354-370. Berlin: Springer.

Krapp, H. G. (2000). Neuronal matched filters for optic flow processing in flying insects. *Int. Rev. Neurobiol.* **44**, 93-120.

Krapp, H. G. and Hengstenberg, R. (1996). Estimation of self-motion by optic flow processing in single visual interneurons. *Nature* **384**, 463-466.

Krapp, H. G. and Hengstenberg, R. (1997). A fast stimulus procedure to determine local receptive field properties of motion-sensitive visual interneurons. *Vision Res.* **37**, 225-234.

Krapp, H. G., Hengstenberg, B. and Hengstenberg, R. (1998). Dendritic structure and receptive-field organization of optic flow processing interneurons in the fly. *J. Neurophysiol.* **79**, 1902-1917.

Krapp, H. G., Hengstenberg, R. and Egelhaaf, M. (2001). Binocular contributions to optic flow processing in the fly visual system. *J. Neurophysiol.* **85**, 724-734.

Land, M. F. (1997). Visual acuity in insects. *Annu. Rev. Entomol.* **42**, 147-177.

Land, M. F. and Collett, T. S. (1974). Chasing behavior of houseflies (*Fannia canicularis*): a description and analysis. *J. Comp. Physiol.* **89**, 331-357.

Land, M. F. and Eckert, H. M. (1985). Maps of the acute zones of fly eyes. *J. Comp. Physiol. A* **156**, 525-538.

Laughlin, S. B. (1981). A simple coding procedure enhances a neuron's information capacity. *Z. Naturforsch. C* **36**, 910-912.

Laughlin, S. B. (1994). Matching coding, circuits, cells, and molecules to signals – general principles of retinal design in the fly's eye. *Prog. Retin. Eye Res.* **13**, 165-196.

Laughlin, S. B., de Ruyter van Steveninck, R. R. and Anderson, J. C. (1998). The metabolic cost of neural information. *Nat. Neurosci.* **1**, 36-41.

Lindemann, J. P., Kern, R., van Hateren, J. H., Ritter, H. and Egelhaaf, M. (2005). On the computations analyzing natural optic flow: quantitative model analysis of the blowfly motion vision pathway. *J. Neurosci.* **25**, 6435-6448.

Maddess, T. and Laughlin, S. B. (1985). Adaptation of the motion-sensitive neuron H-1 is generated locally and governed by contrast frequency. *Proc. R. Soc. Lond. B Biol. Sci.* **225**, 251-275.

McCann, G. D. (1974). Nonlinear identification theory models for successive stages of visual nervous systems of flies. *J. Neurophysiol.* **37**, 869-895.

Nordstrom, K., Barnett, P. D. and O'Carroll, D. C. (2006). Insect detection of small targets moving in visual clutter. *PLoS Biol.* **4**, 378-386.

O'Carroll, D. C. (2001). Motion adaptation and evidence for parallel processing in the lobula plate of the bee-fly *Bombylus major*. In *Motion Vision – Computational, Neural, and Ecological Constraints* (ed. J. M. Zanker and J. Zeil). Berlin: Springer Verlag.

O'Carroll, D. C., Bidwell, N. J., Laughlin, S. B. and Warrant, E. J. (1996). Insect motion detectors matched to visual ecology. *Nature* **382**, 63-66.

O'Carroll, D. C., Laughlin, S. B., Bidwell, N. J. and Harris, R. A. (1997). Spatio-temporal properties of motion detectors matched to low image velocities in hovering insects. *Vision Res.* **37**, 3427-3439.

Reichardt, W., Poggio, T. and Hausen, K. (1983). Figure-ground discrimination by relative movement in the visual-system of the fly. 2. Towards the neural circuitry. *Biol. Cybern.* **46**, 1-30.

Rutowski, R. L. and Warrant, E. J. (2002). Visual field structure in the Empress Leilia, *Asterocampa leilia* (Lepidoptera, Nymphalidae): dimensions and regional variation in acuity. *J. Comp. Physiol. A* **188**, 1-12.

Schuling, F. H., Mastebroek, H. A. K., Bult, R. and Lenting, B. P. M. (1989). Properties of elementary movement detectors in the fly *Calliphora erythrocephala*. *J. Comp. Physiol. A* **165**, 179-192.

Shoemaker, P. A., O'Carroll, D. C. and Straw, A. D. (2001). Implementation of visual motion detection with contrast adaptation. *Proc. SPIE* **4591**, 316-327.

Shoemaker, P. A., O'Carroll, D. C. and Straw, A. D. (2005). Velocity constancy and models for wide-field visual motion detection in insects. *Biol. Cybern.* **93**, 275-287.

Srinivasan, M. V. and Dvorak, D. R. (1980). Spatial processing of visual information in the movement-detecting pathway of the fly: characteristics and functional significance. *J. Comp. Physiol. A* **140**, 1-23.

Srinivasan, M. V., Laughlin, S. B. and Dubs, A. (1982). Predictive coding – a fresh view of inhibition in the retina. *Proc. R. Soc. Lond. B Biol. Sci.* **216**, 427-459.

van Hateren, J. H. (1989). Photoreceptor optics: theory and practice. In *Facets of Vision* (ed. D. G. Stavenga and R. C. Hardie), pp. 74-89. New York: Springer-Verlag.

van Hateren, J. H. (1990). Directional tuning curves, elementary motion detectors, and the estimation of the direction of visual movement. *Vision Res.* **30**, 603-614.

van Hateren, J. H., Hardie, R. C., Rudolph, A., Laughlin, S. B. and Stavenga, D. G. (1989). The bright zone, a specialized dorsal eye region in the male blowfly *Chrysomyia megacephala*. *J. Comp. Physiol. A* **164**, 297-308.

Wagner, H. (1986). Flight performance and visual control of the free-flying housefly, *Musca domestica*. II. Pursuit of targets. *Philos. Trans. R. Soc. Lond. B Biol. Sci.* **312**, 553-579.

Wehrhahn, C. (1979). Sex-specific differences in the chasing behavior of houseflies (Musca). *Biol. Cybern.* **32**, 239-241.

Zanker, J. M., Srinivasan, M. V. and Egelhaaf, M. (1999). Speed tuning in elementary motion detectors of the correlation type. *Biol. Cybern.* **80**, 109-116.